Electronic Journal of Mathematical Analysis and Applications
Vol. 13(2) July 2025, No. 15.
ISSN: 2090-729X (online)
ISSN: 3009-6731(print)
http://ejmaa.journals.ekb.eg/

DYNAMICS OF FOOT-AND-MOUTH DISEASE SPREAD IN A BOVINE POPULATION WITH VACCINATION

H. DJIMRAMADJI, A. S. ABDRAMANE, M. S. DAOUSSA HAGGAR

Abstract. In this paper, we formulate a deterministic model describing the dynamics of foot-and-mouth disease transmission in a cattle population, incorporating the culling policy for infected animals. We compute the basic reproduction number $\mathcal{R}_0$, which enables us to characterize the disease progression while ensuring the positivity of the state variables. We prove that the epidemic can be controlled when $\mathcal{R}_0 < 1$. Consequently, vaccination remains the most effective strategy for controlling and eradicating the disease, as demonstrated by the sensitivity analysis of $\mathcal{R}_0$ and numerical simulations. Parameter estimation is performed to better understand strategies for reducing secondary infections, and theoretical results are supported through numerical simulations. Our findings highlight that effective vaccination provides strong immunity and significantly reduces secondary infections in cattle.

1. Introduction

Foot-and-mouth disease is a highly contagious transboundary viral disease affecting domestic and wild artiodactyl animals, leading to significant economic impacts [14, 25]. The domestic animal species most affected by this disease include cattle, goats, pigs, sheep, and camels [22]. The virus responsible for foot-and-mouth disease is known as the foot-and-mouth virus, an RNA virus belonging to the *Picornaviridae* family and the *Aphtovirus* genus [5]. The foot-and-mouth virus has a capsid formed by an assembly of proteins—VP1, VP2, and VP3—which makes it highly resistant to cold, dry heat (two and a half hours at 70°C and 7 minutes at 105°C), and moist heat (30 minutes at 65°C and 3 minutes at 90°C) [18]. Infection by the virus primarily occurs through the respiratory route. However, the virus is found in all excretions and secretions of infected animals, as well as in milk, food,

2020 *Mathematics Subject Classification.* 34A34, 34D20.
Key words and phrases. Mathematical modeling; foot-and-mouth disease; basic reproduction number; sensitivity analysis; numerical simulation.
Submitted Jan. 8, 2025. Revised June 10, 2025. Accepted Sep. 6, 2025.

water, and any objects that have come into contact with sick animals [22], with an incubation period ranging from 48 hours to 15 days. The likelihood of transmission of foot-and-mouth disease depends on distance: the closer the infectious animals are, the higher the probability of transmission, and vice versa [16].

Cattle are the species most susceptible to the disease. In cattle, foot-and-mouth disease manifests as vesicles in the oral cavity, on the tongue, interdigital areas, the coronary band, and the hooves [18]. It is worth noting that animals recovering from the disease can become asymptomatic carriers of the virus, posing a threat to susceptible, unvaccinated animals [18]. While the vaccination induces antibodies mainly to structural proteins, the presence of antibodies to the non-structural proteins (NSP) is suggestive of infection, a criterion for differentiation of infected from vaccinated animals (DIVA) [25].

The probability of infection varies with distance. Transmission probabilities are as follows: 0.25, 0.13, 0.06, 0.02, and 0.0, corresponding respectively to distances of 0 to 0.5 km, 0.5 to 1 km, 1 to 2 km, 2 to 5 km, and over 5 km [16].

Chad, one of Africa's major livestock-producing countries, has been fighting animal diseases on a large scale. Despite significant resources being allocated, the country's livestock sector faces challenges in combating epizootics. Foot-and-mouth disease remains a severe problem for livestock in Chad. Numerous studies have shown that foot-and-mouth disease is endemic in Chad, with cattle being the most affected species. Although the disease occurs episodically in cattle, its spread varies across regions. For instance, studies conducted in 106 villages revealed a seroprevalence rate of 60% [23]. Research in the Central and Northeastern regions of Chad indicated a 40% seroprevalence rate from 1,520 serum samples (928 cattle, 216 goats, 254 sheep, and 122 camels) [1]. Specifically, seroprevalence rates in cattle over five years old were 78% and 84% in East Batha and West Batha, respectively, and 67% in Wadi Fira for cattle under one year old. These rates were 64% in East Batha and 59% in West Batha [1]. These data highlight the urgent need for solutions to limit new infections.

Foot-and-mouth disease has been the focus of numerous researchers. Some have developed economic models [4, 9, 26], while others have created spatial models [8, 10, 15]. Concerned about ensuring a healthy food supply, Guillaume [13] investigated strategies for optimizing mutualized abattoir funds through a study on the impact of foot-and-mouth disease on agri-food industries. He employed the SIR model [2, 17] while incorporating immunity and vaccination.

Recent studies in sub-Saharan Africa show that FMD has an incubation period of 2-14 days (average 4-6 days), a transmission rate of 0.18-0.32 per day, and morbidity reaching 80-100% in naive herds, with mortality of 2-5% in adults and 20-30% in young animals [20]. Standard vaccines (75-85% efficacy) see their protection drop to 40-50% after 6 months in real conditions [6]. In Chad, the serological prevalence reaches 62% (dominant SAT1 serotype) [19], with an empirical $\mathcal{R}_0$ of 3.2 [21]. These data suggest heterogeneity of transmission (super-shedders), vaccine degradation under pastoral conditions, and seasonality of outbreaks, while calibrating transmission and recovery rates to the observed ranges (0.18-0.32 and 0.1-0.3 per day respectively) for robust biological validation.

The objective of this article is to propose an epidemiological model that takes into account vaccination and culling due to the weakening of cattle by foot-and-mouth disease.

In Section 2, we present the formulation of the model; a comprehensive analysis of the model is provided in Section 3, and finally, numerical simulations are presented in Section 4.

2. Mathematical model formulation

In this section, we formulate the mathematical model describing the progression of the foot-and-mouth disease virus in the cattle population. This model is designed to analyze the spread of foot-and-mouth disease infection within the cattle population, incorporating vaccination, protection, exposure to the disease, and culling policies. The total cattle population is divided into six classes, along with an intermediate class of cattle weakened by the disease that are culled. The model is developed based on the following assumptions:

H_1: Protected individuals are immune to the disease.
H_2: Recovered individuals can become susceptible to reinfection.
H_{3a}: A proportion α of infected individuals weakened by the disease is culled.
H_{3b}: A proportion η of recovered individuals weakened by the disease is culled.

Susceptible individuals are infected at a rate β. A proportion of susceptibles is vaccinated against the infection at a rate δ. Susceptibles who are infected become exposed, reflecting the incubation period of foot-and-mouth disease. The effectiveness of the vaccine is denoted by θ. Specifically, the vaccine effectiveness is calculated as follows [11]:

$$E_V = 1 - \frac{R_V}{R_{NV}} \tag{1}$$

where R_V is the incidence in the vaccinated population, and R_{NV} is the incidence rate (or risk) in the unvaccinated population.

Vaccinated cattle lose their immunity at a rate τ. The class D, representing culled individuals, is not explicitly included in the system of differential equations.

Symbol	Description of model variables
S	Number of susceptibles: individuals at risk of contracting the infection.
E	Number of exposed: individuals exposed to the infection but not yet infectious.
I	Number of infected: individuals infected and capable of transmitting the infection.
V	Number of vaccinated: susceptible individuals vaccinated against the infection.
R	Number of recovered: individuals who have recovered from the infection.
P	Number of protected: vaccinated individuals who are immune to the infection.
D	Number of culled: individuals culled due to weakness caused by the infection.

Table 1. Description of model variables

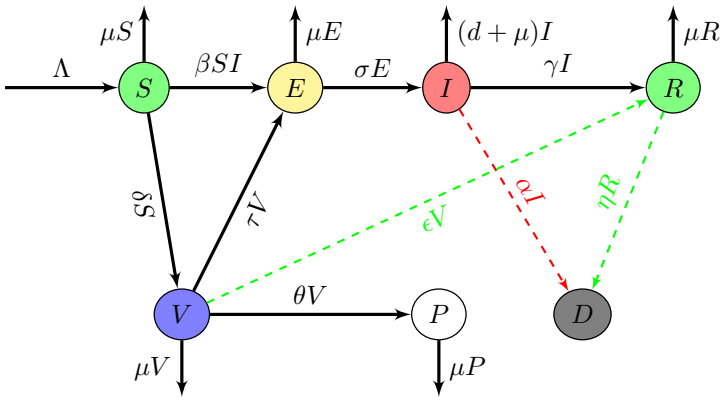

FIGURE 1. Flow diagram of the foot-and-mouth disease model compartments

$$\frac{dS}{dt} = \Lambda - \beta SI - (\delta + \mu)S \tag{2a}$$
$$\frac{dE}{dt} = \beta SI + \tau V - (\sigma + \mu)E \tag{2b}$$
$$\frac{dI}{dt} = \sigma E - (\mu + d + \alpha + \gamma)I \tag{2c}$$
$$\frac{dV}{dt} = \delta S - \tau V - (\mu + \theta + \epsilon)V \tag{2d}$$
$$\frac{dR}{dt} = \gamma I + \epsilon V - (\mu + \eta)R \tag{2e}$$
$$\frac{dP}{dt} = \theta V - \mu P \tag{2f}$$

provided with the initial conditions

$$S(0) > 0, E(0) \geq 0, I(0) \geq 0, V(0) \geq 0, R(0) \geq 0, P(0) \geq 0. \tag{2g}$$

3. Mathematical model analysis

3.1. **Basic analysis.**

3.1.1. *Feasible region of the model.* We assume that all parameters and state variables in system (2) remain positive for all times $t \geq 0$.

Lemma 3.1. *The set*

$$\Omega = \left\{ \mathbf{X} \in \mathbb{R}^6, \mathbf{X}(t) \geq \mathbf{0},\ 0 \leq N(t) \leq \frac{\Lambda}{\mu} \right\} \tag{3}$$

is positively invariant.

Proof. From equation (2a), we have:

$$\frac{dS}{dt} = \Lambda - \beta SI - (\delta + \mu)S$$

with the solution:

$$S(t) = e^{-\int_0^t k_1(x)\,dx}\left[S(0) + \Lambda\int_0^t e^{\int_0^x k_1(s)\,ds}dx\right], \tag{4}$$

where $k_1(t) = \beta I(t) + \delta + \mu$. Since $k_1(t) \geq 0$ and $S(0) \geq 0$, we conclude that $S(t) \geq 0$ for all $t \geq 0$.

For equation (2b):

$$\frac{dE}{dt} = \beta SI + \tau VI - (\sigma + \mu)E,$$

assume, by contradiction, that there exists a time $t_1 > 0$ such that $E(t_1) = 0$, $E'(t_1) < 0$, and $\mathbf{X}(t_1) > \mathbf{0}$. Then, from the equation, we get $E'(t_1) = \beta S(t_1)I(t_1) + \tau V(t_1)I(t_1) > 0$, a contradiction. Thus, $E(t) \geq 0$ for all $t \geq 0$.

From equation (2c):

$$\frac{dI}{dt} = \sigma E - (\mu + d + \alpha + \gamma)I,$$

we get the solution:

$$I(t) = e^{-(\mu+d+\alpha+\gamma)t}\left[I(0) - \frac{\Lambda}{\mu + d + \alpha + \gamma}\right] + \frac{\Lambda}{\mu + d + \alpha + \gamma} \geq 0. \tag{5}$$

Similarly, for $V(t)$:

$$\frac{dV}{dt} = \delta S - \tau VI - (\mu + \theta + \epsilon)V,$$

we have:

$$V(t) = e^{-\int_0^t k_2(x)\,dx}\left[V(0) + \int_0^t \delta S(x)e^{\int_0^x k_2(s)\,ds}dx\right] \geq 0, \tag{6}$$

where $k_2(t) = \tau I(t) + \theta + \mu + \epsilon$.

In the same way:

$$R(t) = e^{-(\mu+\eta)t}\left[R(0) + \int_0^t k_3(x)e^{(\mu+\eta)x}dx\right] \geq 0, \quad P(t) = e^{\mu t}\left[P(0) + \theta\int_0^t V(x)e^{-\mu x}dx\right] \geq 0,$$

where $k_3(t) = \gamma I(t) + \epsilon V(t)$.

Now we show that the total population $N(t)$ is bounded. From the system:

$$\frac{dN}{dt} = \Lambda - \mu N(t) - dI - \eta R \tag{7}$$

$$\leq \Lambda - \mu N(t). \tag{8}$$

Solving this differential inequality, we obtain:

$$0 \leq N(t) \leq e^{-\mu t}\left[N(0) - \frac{\Lambda}{\mu}\right] + \frac{\Lambda}{\mu}.$$

Therefore, as $t \to \infty$:

$$0 \leq N(t) \leq \frac{\Lambda}{\mu}.$$

□

3.1.2. *Disease-Free Equilibrium.* The disease-free equilibrium (DFE) of the model (2), corresponding to the absence of infection in the population, is given by:

$$E_0^* = \left(\frac{\Lambda}{\delta+\mu},\ 0,\ 0,\ \frac{\Lambda\delta}{(\delta+\mu)(\mu+\theta+\epsilon)},\ \frac{\Lambda\delta\epsilon}{(\mu+\epsilon)(\delta+\mu)(\mu+\theta)},\ \frac{\Lambda\delta\theta}{\mu(\delta+\mu)(\mu+\theta)} \right) \tag{9}$$

3.2. **Reproduction number.** We compute the basic reproduction number $\mathcal{R}_0$ following the next-generation matrix approach [24], evaluated at the disease-free equilibrium point E_0^* given in equation (9). We obtain the matrices:

$$F = \begin{pmatrix} 0 & \frac{\Lambda\beta(\mu+\theta+\epsilon)+\Lambda\delta\tau}{(\delta+\mu)(\mu+\theta+\epsilon)} \\ 0 & 0 \end{pmatrix}, \quad V = \begin{pmatrix} \mu+\sigma & 0 \\ -\sigma & \mu+d+\alpha+\gamma \end{pmatrix},$$

with inverse:

$$V^{-1} = \begin{pmatrix} \frac{1}{\mu+\sigma} & 0 \\ \frac{\sigma}{(\mu+\sigma)(\mu+d+\alpha+\gamma)} & \frac{1}{\mu+d+\alpha+\gamma} \end{pmatrix}.$$

The next-generation matrix is given by:

$$FV^{-1} = \begin{pmatrix} \frac{\Lambda\beta\sigma(\mu+\theta+\epsilon)+\Lambda\delta\tau\sigma}{(\mu+\sigma)(\delta+\mu)(\mu+\theta+\epsilon)(\mu+d+\alpha+\gamma)} & \frac{\Lambda\beta(\mu+\theta+\epsilon)+\Lambda\delta\tau}{(\delta+\mu)(\mu+\theta+\epsilon)(\mu+d+\alpha+\gamma)} \\ 0 & 0 \end{pmatrix}.$$

Hence, the basic reproduction number is:

$$\mathcal{R}_0 = \frac{\Lambda\beta\sigma(\mu+\theta+\epsilon)+\Lambda\delta\tau\sigma}{(\mu+\sigma)(\delta+\mu)(\mu+\theta+\epsilon)(\mu+d+\alpha+\gamma)}. \tag{10}$$

We analyze the sensitivity of $\mathcal{R}_0$ with respect to model parameters:

$$\begin{aligned}
&\frac{\partial\mathcal{R}_0}{\partial\Lambda} = \frac{\beta(\mu+\theta+\epsilon)+\delta\tau}{(\mu+\sigma)(\delta+\mu)(\mu+\theta+\epsilon)(\mu+d+\alpha+\gamma)} > 0,\\
&\frac{\partial\mathcal{R}_0}{\partial\beta} = \frac{\Lambda\sigma(\mu+\theta+\epsilon)}{(\mu+\sigma)(\delta+\mu)(\mu+\theta+\epsilon)(\mu+d+\alpha+\gamma)} > 0,\\
&\frac{\partial\mathcal{R}_0}{\partial\gamma} = \frac{\partial\mathcal{R}_0}{\partial d} = \frac{\partial\mathcal{R}_0}{\partial\alpha} = -\frac{\Lambda\beta\sigma(\mu+\theta+\epsilon)+\Lambda\delta\tau\sigma}{(\mu+\sigma)(\delta+\mu)(\mu+\theta+\epsilon)(\mu+d+\alpha+\gamma)^2} < 0,\\
&\frac{\partial\mathcal{R}_0}{\partial\tau} = \frac{\Lambda\delta\sigma}{(\mu+\sigma)(\delta+\mu)(\mu+\theta+\epsilon)(\mu+d+\alpha+\gamma)} > 0,\\
&\frac{\partial\mathcal{R}_0}{\partial\sigma} = \frac{(\Lambda\beta(\mu+\theta+\epsilon)+\Lambda\delta\tau)(\mu-\sigma)}{(\mu+\sigma)^2(\delta+\mu)(\mu+\theta+\epsilon)(\mu+d+\alpha+\gamma)},\\
&\frac{\partial\mathcal{R}_0}{\partial\theta} = \frac{\Lambda\sigma\left[\beta(\mu+\theta+\epsilon)+\delta\tau\right](\mu-\theta)}{(\mu+\sigma)(\delta+\mu)(\mu+\theta+\epsilon)^2(\mu+d+\alpha+\gamma)} < 0,\\
&\frac{\partial\mathcal{R}_0}{\partial\delta} = \frac{\Lambda\tau\sigma(\mu+\delta)-\Lambda\delta\tau\sigma-\Lambda\beta\sigma(\mu+\theta+\epsilon)}{(\mu+\sigma)(\delta+\mu)^2(\mu+\theta+\epsilon)(\mu+d+\alpha+\gamma)} < 0,\\
&\frac{\partial\mathcal{R}_0}{\partial\mu} < 0 \text{ (complex expression, but strictly negative)},\\
&\frac{\partial\mathcal{R}_0}{\partial\eta} = 0.
\end{aligned}$$

Interpretation:

(1) **No effect from η:** Since $\partial\mathcal{R}_0/\partial\eta = 0$, the culling of recovered individuals has no impact on disease transmission. However, separating them from healthy individuals remains advisable.
(2) **Positive influence on $\mathcal{R}_0$:** Increasing Λ, β, or τ raises $\mathcal{R}_0$. Thus, reducing the recruitment of unvaccinated susceptibles, minimizing contact between susceptible and infected cattle, and preventing vaccine efficacy loss are key strategies.
(3) **Negative influence on $\mathcal{R}_0$:** Increasing vaccination rate δ, vaccine efficacy θ, recovery rate γ, and loss rate ϵ decreases $\mathcal{R}_0$. Hence, vaccination campaigns should focus on improving these factors.
(4) **Mortality-related effects:** Increasing disease-induced mortality d, slaughter rate α, or natural death rate μ reduces $\mathcal{R}_0$, but these are economically and ethically undesirable strategies.
(5) **Impact of σ:** If $\mu < \sigma$, then $\frac{\partial\mathcal{R}_0}{\partial\sigma} < 0$, which helps reduce disease spread. However, for $\mu > \sigma$, we get $\frac{\partial\mathcal{R}_0}{\partial\sigma} > 0$, implying acceleration of infection. Therefore, reducing the progression from exposed to infectious (via vaccination) is one of the most effective strategies.

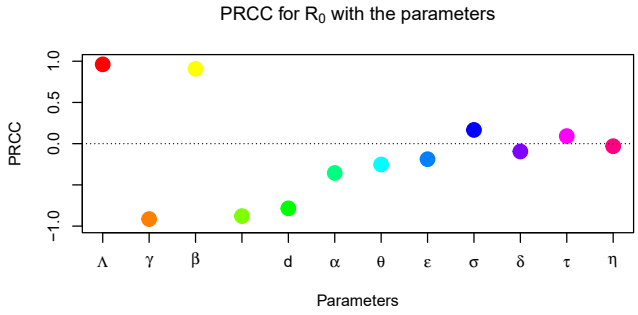

FIGURE 2. PRCC for $\mathcal{R}_0$

Interpretation: Figure (2) shows that parameters far from the origin are highly sensitive to changes in $\mathcal{R}_0$. However, it will be necessary to reduce the recruitment of unvaccinated susceptibles and decrease the infection rate. Similarly, the recovery rate γ of the infected individuals should be increased through vaccination or treatment in order to reduce new infections.

3.3. **Stability of the disease-free equilibrium point.**

3.3.1. *Local stability of the disease-free equilibrium point.* Let us define the matrix $M = F - V$ as:

$$M = \begin{pmatrix} -(\mu+\sigma) & \dfrac{\Lambda\beta(\mu+\theta+\epsilon)+\Lambda\delta\tau}{(\delta+\mu)(\mu+\theta+\epsilon)} \\ \sigma & -(\mu+d+\alpha+\gamma) \end{pmatrix} \tag{11}$$

which is a square matrix of order 2. The determinant of M can be expressed as: $\det(M) = \lambda_1\lambda_2$, where λ_1 and λ_2 are the eigenvalues of M. According to [Theorem

2, [24]], the system exhibits two equilibrium states when:

$$\mathcal{R}_0 > 1 \Longleftrightarrow det(M) < 0, \quad \mathcal{R}_0 < 1 \Longleftrightarrow det(M) > 0$$

.

Theorem 3.1. *The disease-free equilibrium point E_0^* is locally asymptotically stable if $\mathcal{R}_0 < 1$, otherwise unstable.*

Proof. The Jacobian matrix for the disease-free equilibrium point (9) is:

$$J = \left(\begin{array}{ccc|ccc} -(\mu+\delta) & 0 & -\frac{\Lambda\beta}{\delta+\mu} & 0 & 0 & 0 \\ \hline 0 & -(\mu+\sigma) & \frac{\Lambda\beta(\mu+\theta+\epsilon)+\Lambda\delta\tau}{(\delta+\mu)(\mu+\theta+\epsilon)} & 0 & 0 & 0 \\ 0 & \sigma & -(\mu+d+\alpha+\gamma) & 0 & 0 & 0 \\ \hline \delta & 0 & -\frac{\Lambda\tau\delta}{(\delta+\mu)(\mu+\theta+\epsilon)} & -(\mu+\theta+\epsilon) & 0 & 0 \\ 0 & 0 & \gamma & \epsilon & -(\mu+\eta) & 0 \\ 0 & 0 & 0 & \theta & 0 & -\mu \end{array}\right) \tag{12}$$

and

$$J' = \begin{pmatrix} -\mu-\sigma & \frac{\Lambda\beta(\mu+\theta+\epsilon)+\Lambda\delta\tau}{(\delta+\mu)(\mu+\theta+\epsilon)} \\ \sigma & -(\mu+d+\alpha+\gamma) \end{pmatrix}.$$

The other eigenvalues of the Jacobian matrix J calculated at the disease-free equilibrium point (9) are $\lambda_1 = -(\mu+\sigma)$, $\lambda_4 = -(\mu+\theta+\epsilon)$, $\lambda_5 = -(\mu+\eta)$, and $\lambda_6 = -\mu$, which are negative except for those of the matrix J'. We note that $J' = M$. Therefore,

$$\lambda_3 + \lambda_2 = -(\alpha+d+\gamma+2\mu) \tag{13}$$

$$\lambda_3 \cdot \lambda_2 = (\mu+\sigma)(\mu+d+\alpha+\gamma)(1-\mathcal{R}_0) \tag{14}$$

Using the Routh-Hurwitz criterion [12] and [24], if $\mathcal{R}_0 < 1$, the disease-free equilibrium point E_0^* is locally asymptotically stable. □

3.3.2. *Global stability of the disease-free equilibrium point.*

Theorem 3.2. *The disease-free equilibrium point E_0^* is globally asymptotically stable if $\mathcal{R}_0 < 1$ on the domain*

$$\Omega_1 = \left\{(S,V) \in \mathbb{R}^2, 0 \le S(t) \le \frac{\Lambda}{\mu+\delta}, 0 \le V(t) \le \frac{\Lambda\delta}{(\mu+\delta)(\mu+\theta+\epsilon)}\right\}.$$

Proof. (1) For $E = I = 0$, we obtain, by solving:

$$S(t) = e^{-(\delta+\mu)t}\left(S(0) - \frac{\Lambda}{\delta+\mu}\right) + \frac{\Lambda}{\delta+\mu}$$

$$V(t) = e^{-(\mu+\theta+\epsilon)t}\left(V(0) - \frac{\Lambda\delta}{(\delta+\mu)(\mu+\theta+\epsilon)}\right) + \frac{\Lambda\delta}{(\delta+\mu)(\mu+\theta+\epsilon)} + \frac{\delta}{\theta-\delta}\left(S(0) - \frac{\Lambda}{\delta+\mu}\right)(e^{-(\mu+\delta)t} - e^{-(\mu+\theta+\epsilon)t})$$

$$R(t) = \left(R(0) - \frac{\Lambda\delta\epsilon}{(\mu+\delta)(\mu+\theta+\epsilon)(\mu+\eta)}\right)e^{-(\mu+\eta)t} + h_1(t) + \frac{\Lambda\delta\epsilon}{(\mu+\delta)(\mu+\theta+\epsilon)(\mu+\eta)}$$

$$P(t) = \left(P(0) - \frac{\Lambda\delta\theta}{\mu(\delta+\mu)(\mu+\theta+\epsilon)}\right)e^{-\mu t} + h_2(t) + \frac{\Lambda\delta\theta}{\mu(\delta+\mu)(\mu+\theta+\epsilon)}$$

where

$$h_1(t) = \frac{\delta\theta}{\theta-\delta}\left(S(0)-\frac{\Lambda}{\delta+\mu}\right)(e^{-(\mu+\theta+\epsilon)t}-e^{-(\mu+\eta)t}) + \frac{\epsilon\delta}{\theta+\epsilon-\delta}\left(S(0)-\frac{\Lambda}{\mu+\delta}\right)\left[-\frac{1}{\eta-\delta}(e^{-(\mu+\delta)t}-e^{-(\mu+\eta)t})+\frac{1}{\theta+\epsilon-\eta}(e^{-(\mu+\theta+\epsilon)t}-e^{-(\mu+\eta)t})\right],$$

$$h_2(t) = \frac{\theta}{\theta+\epsilon}\left(V(0)-\frac{\Lambda\delta}{(\delta+\mu)(\mu+\theta+\epsilon)}\right)\left(e^{-\mu t}-e^{-(\mu+\theta+\epsilon)t}\right) + \frac{\delta\theta}{\theta+\epsilon-\delta}\left(S(0)-\frac{\Lambda}{\mu+\delta}\right)\left[\frac{1}{\delta}(e^{-\mu t}-e^{-(\mu+\delta)t})+\frac{1}{\theta+\epsilon}(e^{-(\mu+\theta+\epsilon)t}-e^{-\mu t})\right].$$

Taking the limit as $t\to\infty$, we obtain:

$$\begin{aligned}
\lim_{t\to\infty} S(t) &= \frac{\Lambda}{\delta+\mu},\\
\lim_{t\to\infty} V(t) &= \frac{\Lambda\delta}{(\delta+\mu)(\mu+\theta+\epsilon)},\\
\lim_{t\to\infty} R(t) &= \frac{\Lambda\delta\epsilon}{(\mu+\epsilon)(\delta+\mu)(\mu+\theta)},\\
\lim_{t\to\infty} P(t) &= \frac{\Lambda\delta\theta}{\mu(\delta+\mu)(\mu+\theta)}.
\end{aligned}$$

Thus, the disease-free equilibrium point E_0^* is globally stable.

(2) Let g_1 and g_2 be the functions of the infected variables defined by:

$$g_1 = \beta SI + \tau VI - (\sigma+\mu)E \tag{15}$$

$$g_2 = \sigma E - (\mu+d+\alpha+\gamma)I \tag{16}$$

We define:

$$A = \frac{\partial(g_1,g_2)}{\partial(E,I)}$$

At the disease-free equilibrium point, we obtain the matrix:

$$A = \begin{pmatrix} -(\sigma+\mu) & \frac{\Lambda\beta}{\delta+\mu}+\frac{\Lambda\tau}{(\delta+\mu)(\mu+\theta)} \\ \sigma & -(\mu+d+\alpha+\gamma)\end{pmatrix}$$

and

$$\begin{aligned}
\hat{G}(E,I) &= A\begin{pmatrix}E\\I\end{pmatrix}-\begin{pmatrix}g_1\\g_2\end{pmatrix}\\
&= \begin{pmatrix}\beta\left(\frac{\Lambda}{\delta+\mu}-S\right)I+\tau\left(\frac{\Lambda\delta}{(\delta+\mu)(\mu+\theta+\epsilon)}-V\right)I\\ 0\end{pmatrix}
\end{aligned}$$

S, E, and I are positive, and E_0^* is globally stable if and only if:

$$0\le S(t)\le\frac{\Lambda}{\mu+\delta} \quad\text{and}\quad 0\le V(t)\le\frac{\Lambda\delta}{(\mu+\delta)(\mu+\theta+\epsilon)}.$$

According to the Castillo-Chavez theorem [7], E_0^* is globally asymptotically stable on

$$\Omega_1 = \left\{(S,V)\in\mathbb{R}^2, 0\le S(t)\le\frac{\Lambda}{\mu+\delta}, 0\le V(t)\le\frac{\Lambda\delta}{(\mu+\delta)(\mu+\theta+\epsilon)}\right\}.$$

□

4. Computational investigation

This part of our work is dedicated to the estimation of parameters and the numerical simulation of the studied model in order to understand the predictions of foot-and-mouth disease (FMD) transmission in cattle.

4.1. **Parameter values.** All parameters studied in this model are of critical importance. The numerical values of some parameters are given with their sources, while for the other parameters, we have assumed their values as shown in Table 3.

Symbol	Description of model parameters
Λ	Rate of entry of new individuals into the susceptible population
β	Transmission rate of infection from infectious to susceptible individuals
γ	Recovery rate of infectious individuals
α	Mortality rate of slaughtered infectious individuals
δ	Rate at which susceptible individuals are vaccinated
τ	Rate of loss of protection provided by the vaccine
σ	Rate of progression from exposed to infectious individuals
θ	Vaccine efficacy rate
η	Mortality rate of slaughtered recovered individuals
μ	Natural mortality rate of cattle
d	Mortality rate due to the disease
ϵ	Recovery rate of vaccinated cattle

Table 2. Description of the parameters used in the model. Each symbol represents a specific epidemiological or demographic factor involved in the dynamics of foot-and-mouth disease.

Symbol	Interval	Value	Unit	Source
Λ	50-150	50	day^{-1}	Assumed
β	0.18-0.32	0.21	day^{-1}	[3]
γ	0.1-0.3	0.246	day^{-1}	[3]
α	0.001-0.2	0.1154	day^{-1}	Assumed
δ	0.001-0.2	0.1246	day^{-1}	Assumed
τ	0.00001-0.03	0.01346	day^{-1}	Assumed
σ	0.001-0.2	0.1714	day^{-1}	Assumed
θ	0.2-0.85	0.6871	day^{-1}	[11]
η	0.00001-0.1	0.00123	day^{-1}	Assumed
μ	0.001-0.2	0.124	day^{-1}	[3]
d	0.00001-0.25	0.003	day^{-1}	Assumed
ϵ	0.00001-0.01	0.00016	day^{-1}	[3]

Table 3. Parameter values used in the model, including their respective intervals, fixed values, units, and sources. Parameters without a cited source are assumed for simulation purposes.

4.2. **Numerical simulation.** We present numerical simulations of the model in (2) to analyze foot-and-mouth disease transmission dynamics. The simulations examine vaccination effects on susceptible cattle recruitment, infectious cattle recovery, and the impact of animal slaughter on viral evolution, with all results displayed on a monthly timescale.

Figures 3 show rapid disease spread within the cattle population. The left figure ($\sigma < \mu$, $\mathcal{R}_0 = 6.1484$) demonstrates high infection rates where infectious individuals dominate, while the right figure ($\sigma > \mu$, $\mathcal{R}_0 = 5.0757$) shows exposed individuals increasing rapidly. In both cases, vaccination reduces but does not eliminate infections, leading to endemic persistence.

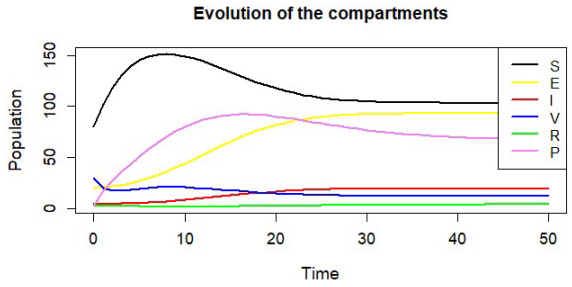

FIGURE 3. Disease dynamics with $\sigma < \mu$ ($\mathcal{R}_0 = 6.1484$). Vaccination reduces transmission but fails to achieve disease elimination

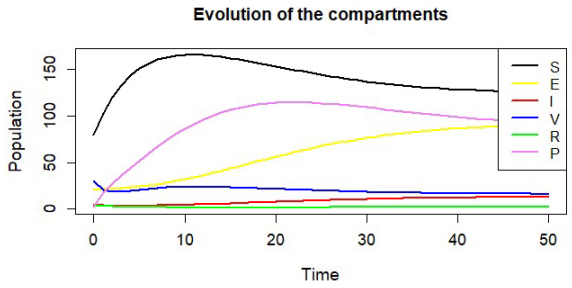

FIGURE 4. Disease dynamics with $\sigma > \mu$ ($\mathcal{R}_0 = 5.0757$). Vaccination reduces transmission but fails to achieve disease elimination

Figure 5 presents a controlled outbreak scenario ($\mathcal{R}_0 = 0.014$) where vaccination significantly reduces transmission. In this case, slaughter policies show minimal impact, and the disease is eventually eradicated through vaccine-induced immunity.

Figure 6 demonstrates that vaccination with at least 75% efficacy leads to complete disease elimination within 30 months. The results show effective protection of the cattle population and sustained disease-free conditions when this vaccination threshold is maintained.

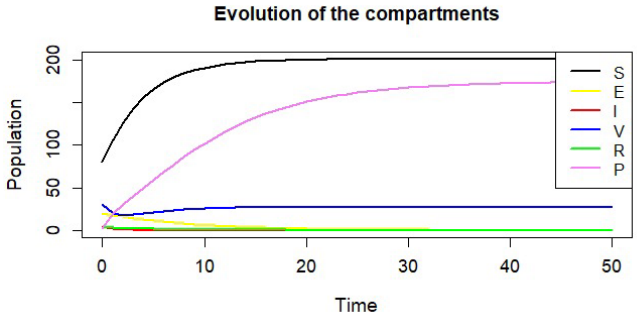

FIGURE 5. Disease elimination under effective vaccination ($\mathcal{R}_0 = 0.014$). Parameters: $\beta = 0.0012$, $\tau = 0.001346$, $\sigma = 0.001714$, $\theta = 0.7871$.

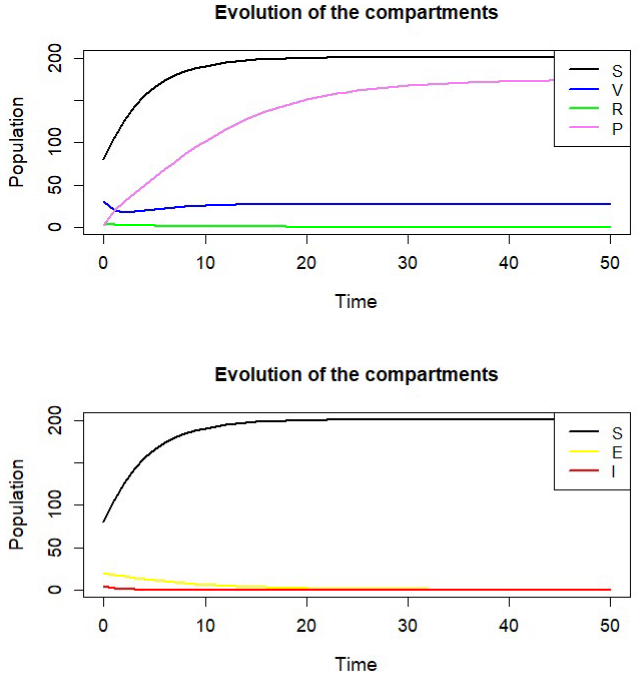

FIGURE 6. Population dynamics with $\mathcal{R}_0 < 1$. Vaccination ($E_V \geq 75\%$) achieves disease elimination within 30 months.

5. CONCLUSION

We developed a deterministic ordinary differential equation model with initial conditions to analyze foot-and-mouth disease dynamics incorporating vaccination. Our analysis established both local and global stability of the disease-free equilibrium through examination of the basic reproduction number $\mathcal{R}_0$ [24]. Parameter

estimation enabled the evaluation of strategies for mitigating secondary infections, while numerical simulations validated our theoretical findings. These results demonstrate that effective vaccination plays a pivotal role in establishing robust immunity and substantially decreasing secondary transmission rates.

Given Chad's heavy reliance on pastoral livestock production systems, future research should employ metapopulation modeling approaches to elucidate disease spread patterns during animal movements. Additionally, cost-effectiveness analyses of treatment strategies will be essential for optimizing animal healthcare expenditures while maintaining disease control efficacy.

While our deterministic framework provides key insights, future work could integrate:

Data assimilation from mobile livestock surveillance;

This interdisciplinary approach would bridge the gap between theoretical rigor and field applicability in Chad's pastoral context.

Conflict of interest

The authors declare none.

References

[1] A. I. Abdel-Aziz. Épidémiologie moléculaire de la fièvre aphteuse en afrique subsaharienne: cas du tchad, 2018. Thèse, AgroParisTech.

[2] A.S Abdramane, H Djimramadji, and M.S Daoussa Haggar. Study of the dynamics of hiv-cholera co-infection in a mathematical model. *Electronic Journal of Mathematical Analysis and Applications*, 13(1):1–11, 2025.

[3] E. Ahmed, A. S. Hegazi, and A. S. Elgazzar. An epidemic model on small-world networks and ring vaccination. *Physica A*, 324:402–407, 2003.

[4] ANONYMOUS. Estudio de pérdidas de producción y productividad in ganado con fiebre aftosa, 1984. Ministry of Agriculture, Brazil / Inter-American Development Bank / Pan American Health Organization, PANAFTOSA, Rio de Janeiro, 78pp.

[5] M. Bertognoli, A. Milon, and M. Schrlcher. Conférence sur la fièvre aphteuse, 2001. Toulouse, ENVT, 27 mars.

[6] B.M. Bronsvoort et al. Field effectiveness of fmd vaccination in pastoral herds. *Frontiers in Veterinary Science*, 10:1125023, 2023. Efficacité vaccinale en conditions réelles.

[7] C. Castillo-Chavez, Z. Feng, and W. Huang. On the computation of r_0 and its role on global stability. In *Mathematical approaches for emerging and re-emerging infectious diseases: an introduction*, volume 125, pages 31–65. The IMA Volumes in Mathematics and Its Applications, 2002.

[8] S. M. Daggupaty and R. F. Sellers. Airborne spread of foot-and-mouth disease in saskatchewan. *Canadian Journal of Veterinary Epidemiology Research*, 54:465–468, 1990.

[9] A. A. Djikhuizen. Epidemiological and economic evaluation of fmd control strategies in the netherlands. *Netherlands Journal of Agricultural Science*, 37:1–12, 1989.

[10] A. I. Donaldson, M. Lee, and M. Shimshony. A possible airborne transmission of foot and mouth disease virus from jordan to israel: a simulated computer analysis. *Israel Journal of Veterinary Medicine*, 4(2):92–96, 1988.

[11] G. Ferrari, D. Paton, S. Duffy, C. Bartels, and T. Knight-Jones. Reproduction numbers and sub-threshold endemic equilibria for compartmental models of disease transmission. *Mathematical Biosciences*, 180(1-2):29–48, 2002. FAO and OIE.

[12] F. R. Gantmacher. *The theory of matrices*. AMS Chelsea Publishing, Providence, 1998. Translated from the Russian by K. A. Hirsch, reprint of the 1959 translation.

[13] N. Guillaume. Impact de la fièvre aphteuse sur les industries agroalimentaires, perspectives de gestion, jan 2011.

[14] A. Habou. *Contribution à l'étude de la fièvre aphteuse en Afrique de l'Ouest: le cas particulier du Niger*. Thèse de doctorat vétérinaire, Université de Dakar, année à préciser.

[15] M. E. Hugh-Jones. A simulation spatial model of the spread of foot-and-mouth disease through the primary movement of milk. *Journal of Hygiene*, 77:1–9, 1976.
[16] H Kabore. *Modélisation mathématique de la transmission locale du virus de la fièvre aphteuse*. PhD thesis, Université de Montréal, 2006. Médecine vétérinaire.
[17] W. O. Kermack and Anderson G McKendrick. A contribution to the mathematical theory of epidemics. *Proceedings of the royal society of london. Series A, Containing papers of a mathematical and physical character*, 115(772):700–721, 1927.
[18] J Maupone. Résurgence de la fièvre aphteuse en europe en 2001. *Médecine vétérinaire et santé animale*, 2002. dumas-04653282.
[19] S. Molia et al. Foot-and-mouth disease in chad: seroprevalence and virus characterization. *Transboundary and Emerging Diseases*, 67(2):549–560, 2020. Prévalence au Tchad et sérotypes dominants.
[20] W. Molla et al. Extended excretion of foot-and-mouth disease virus in persistently infected african buffalo. *Veterinary Microbiology*, 265:109319, 2022. Période d'incubation et excrétion virale.
[21] A. Namatovu et al. Transmission dynamics of foot-and-mouth disease in east africa. *PLoS Computational Biology*, 17(8):e1009321, 2021. Taux de transmission et R0 empirique.
[22] Oie. Fièvre aphteuse. https://www.oie.int/fr/sante-animale-dans-le-monde/statuts-officiels-des-maladies. Consulté le 09 juin 2025.
[23] M Ouagal, Emiliana Brocch, Grazioli, Adel B. Y, Keith Sumption, P. Hendrikx, Dirk Berkvens, and Claude Saegerman. Evaluation de la sensibilité du réseau d'épidémiosurveillance des maladies animales au tchad pour la surveillance de la fièvre aphteuse. *Epidémiologie et Santé Animale*, 72, 2007.
[24] P. van den Driessche and J. Watmough. Vaccination contre la fièvre aphteuse et suivi post-vaccination, 2020. Elsevier.
[25] H. B. Ranjitha, V. V. Dhanesh, M. Hosamani, and B. P Sreenivasa. Thermostable negative-marker foot-and-mouth disease virus serotype o induces protective immunity in guinea pigs. *Applied microbiology and biotechnology*, 4(107), 2023.
[26] P. Trapman, R. Meester, and H. Heesterbeek. A branching model for the spread of infectious animal disease in varying environments. `http://www.cs.vunl/-rmeester/preprints/epiart-pdf`, 2003.

Djimramadji Hippolyte
Laboratory of Mathematical Modeling, Computer Science, Applications and Simulation (L2MIAS), University of N'Djamena, N'Djamena, Chad
Email address: `hippolytedjimramadji@gmail.com`

Abdramane Annour Saad
Laboratory of Mathematical Modeling, Computer Science, Applications and Simulation (L2MIAS), University of N'Djamena, N'Djamena, Chad
Email address: `annoursaadabdramane31@gmail.com, saad@abdramane.com`

Mahamat Saleh Daoussa Haggar
Laboratory of Mathematical Modeling, Computer Science, Applications and Simulation (L2MIAS), University of N'Djamena, N'Djamena, Chad
Email address: `msdhaggar@gmail.com`